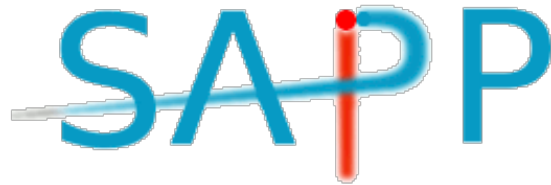


# **20<sup>th</sup> Symposium on Application of Plasma Processes**



## **COST TD1208 Workshop on Application of Gaseous Plasma with Liquids**

### **Book of Contributed Papers**

Tatranská Lomnica, Slovakia  
17-22 January, 2015

Edited by P. Papp, J. Országh, L. Moravský, A. Ribar, Š. Matejčík

Book of Contributed Papers: 20th Symposium on Application of Plasma Processes and COST TD1208 Workshop on Application of Gaseous Plasma with Liquids, Tatranská Lomnica, Slovakia, 17-22 January 2015

Symposium organised by Department of Experimental Physics, Faculty of Mathematics, Physics and Informatics, Comenius University in Bratislava; Society for Plasma Research and Applications, in hotel Slovan, Tatranská Lomnica, Slovakia, 17-22 January 2015

Editors: P. Papp, J. Országh, L. Moravský, A. Ribar, Š. Matejčík

Publisher: Department of Experimental Physics, Faculty of Mathematics, Physics and Informatics, Comenius University in Bratislava (Slovakia); Society for Plasma Research and Applications in cooperation with Library and Publishing Centre CU, Bratislava, Slovakia

Issued: January 2015, Bratislava, first issue

Number of pages: 341

URL: <http://neon.dpp.fmph.uniba.sk/sapp>

ISBN: 978-80-8147-027-1

EAN: 9788081470271

## Contents

COST TD1208 Workshop on Application of Gaseous Plasma with Liquids .....	11
<b>IL-01 INFLUENCE OF PLASMA-TREATED LIQUIDS ON STRUCTURE AND FUNCTION OF LIPID MEMBRANES</b>	
<b><u>M. U. Hammer</u></b> , S. Kupsch, E. Forbrig, H. Jablonowski, K. Masur, K.-D. Weltmann, A. Beerlink, T. Gutschmann, S. Reuter .....	12
<b>IL-02 WATER ELECTROSPRAY THROUGH AIR CORONA AND SPARK DISCHARGES AND INDUCED WATER CHEMISTRY</b>	
B. Pongráč, V. Martišovits, M. Janda, B. Tarabová, K. Hensel, <b><u>Z. Machala</u></b> .....	13
<b>IL-03 ACTIVE BUT NONCULTURABLE STATE OF ESCHERICHIA COLI INDUCED BY PLASMA GENERATED IN GAS AND LIQUID PHASE</b>	
<b><u>E. Dolezalova</u></b> , V. Prukner, P. Lukes, M. Simek .....	17
<b>IL-04 NANOPARTICLE GENERATION BY PULSED LASER ABLATION IN LIQUID</b>	
<b><u>F. Brandi</u></b> .....	22
<b>HT-01 ELEMENTARY PROCESSES IN ARGON COVERED CLUSTERS - THE WAY TO NOVEL PLASMA CHEMISTRY?</b>	
<b><u>J. Kocisek</u></b> , J. Lengyel, P. Slavicek, M. Farnik .....	23
<b>HT-02 DETECTION OF ROS/RNS IN WATER ACTIVATED BY AIR TRANSIENT SPARK DISCHARGE</b>	
<b><u>B. Tarabová</u></b> , P. Lukeš, K. Tarabová, K. Hensel, L. Šikurová, Z. Machala .....	27
<b>HT-03 DEGRADATION OF AMOXICILLIN IN WATER TREATED WITH DBD PLASMA</b>	
<b><u>T. Izdebski</u></b> , E. Ceriani, E. Marotta, C. Paradisi, M. Dors .....	32
20 <sup>th</sup> Symposium on Application of Plasma Processes .....	38
<b>HT-04 ELECTRON AFFINITY EVALUATION FROM NEGATIVE ION MASS SPECTROMETRY DATA</b>	
<b><u>N. Asfandiarov</u></b> , S. Pshenichnyuk, A. Vorob'ev, E. Nafikova, Y. Elkin, A. Modelli .....	39
<b>HT-05 ANION CHEMISTRY ON TITAN: A POSSIBLE ROUTE TO LARGE HYDROCARBONS</b>	
<b><u>J. Žabka</u></b> , M. Polášek, C. Romanzin, C. Alcaraz .....	43
<b>IL-05 STUDY OF PLASMA-CHEMISTRY PROCESSES IN ATMOSPHERIC PRESSURE PLASMAS: ABSOLUTE DENSITY MEASUREMENTS OF RADICALS, VUV SPECTROSCOPY AND SIMULATIONS</b>	
<b><u>J. Benedikt</u></b> , K. Rügner, S. Schneider, S. Große-Kreul, V. Layes, G. Willems, M. Hefny, S. Hübner, A. von Keudell .....	44
<b>IL-06 SPATIOTEMPORAL IMAGING OF SELF-PULSING NANOSECOND DISCHARGES</b>	
<b><u>M. Janda</u></b> , K. Hensel, A. Buček, V. Martišovits, Z. Machala .....	50
<b>HT-06 FAST NEUTRALS AND ENERGY-DEPENDENT SECONDARY ELECTRON EMISSION COEFFICIENTS IN PIC/MCC SIMULATIONS OF CAPACITIVELY COUPLED PLASMAS</b>	
<b><u>A. Derzsi</u></b> , I. Korolov, E. Schüngel, Z. Donkó, J. Schulze .....	56

# SPATIOTEMPORAL IMAGING OF SELF-PULSING NANOSECOND DISCHARGES

Mário Janda<sup>1</sup>, Karol Hensel<sup>1</sup>, Andrej Buček<sup>1</sup>, Viktor Martišovič<sup>1</sup>, Zdenko Machala<sup>1</sup>

<sup>1</sup>*Faculty of Mathematics, Physics and Informatics, Comenius University, Mlynská dolina, 84248  
Bratislava, Slovakia  
E-mail: janda@fmph.uniba.sk*

A streamer-to-spark transition in a self-pulsing transient spark (TS) discharge of positive polarity was investigated using a fast iCCD camera. The entire temporal evolution of the TS, including the primary streamer, the secondary streamer, and the transition to spark was recorded with 2 ns time resolution. Additionally, a streak camera like images were obtained using spatiotemporal reconstruction of the discharge emission detected by a photomultiplier tube with light collection system placed on a micrometric translation stage. With increasing TS repetition frequency  $f$  (from ~1 to 6 kHz), the increase of the propagation velocity of both the primary and the secondary streamer was observed. Accelerating propagation of the secondary streamer crossing the entire gap could explain short streamer-to-spark transition times  $\tau$  (~100 ns) at  $f$  above ~3 kHz. Acceleration of the primary and secondary streamers and shortening of  $\tau$  with increasing  $f$  was attributed to the memory effect composed of pre-heating, pre-ionization, or gas composition changes induced by the previous TS pulses.

## 1. Introduction

Streamer-to-spark transition leading to the gas breakdown is a critical issue when working with various atmospheric pressure electrical discharges, as well as in the design of high voltage (HV) devices and switches. The most typical approach preventing the spark breakdown is to maintain the low temperature plasma character and to prevent excessive discharge currents. On the other hand, periodic streamer-to-spark transition with restricted spark phase can bring multiple benefits in various applications of non-thermal plasmas, such as local and transient elevation of the gas temperature, formation of hydrodynamic expansion, producing high concentrations of reactive species, etc. [1-5]. A relatively simple discharge operating with periodic streamer-to-spark transition and controlled spark phase is the transient spark (TS) discharge [5-7].

The TS is typically generated in atmospheric pressure air or other gases between metal electrodes in point-to-plane configuration with distance  $d = 4-10$  mm, by a DC HV power supply connected to the electrodes via a series resistor  $R = 5-10$  M $\Omega$  (Figure 1). Both polarities are possible, but here we present a study of positive polarity TS discharge with anode as the HV point electrode. The TS is initiated by a primary streamer creating a relatively conductive plasma bridge between the electrodes. It enables partial discharging of the internal capacity  $C$  of the electric circuit, and a local gas heating inside the plasma channel [7]. When the gas temperature  $T$  inside the plasma channel reaches ~1000 K, a very short (~10-100 ns) high current (>1 A) spark current pulse appears (Figure 2).

During the spark phase lasting only a few tens of nanoseconds, the internal circuit capacity  $C$  discharges completely and the potential  $V$  on the HV electrode drops to almost zero. Transition to steady-state arc after the spark is restricted by the ballast resistor  $R$ , and the discharge starts to decay after the  $V$  drop. Eventually, the potential  $V$  starts to gradually increase as the capacity  $C$  recharges.

A new TS pulse, initiated by a new primary streamer, occurs when  $V$  reaches the breakdown voltage again. The TS is thus characteristic of the repetitive primary streamer formation transiting to the spark, with the frequency  $f$  in the kHz range. The increase of  $f$ , achieved by increasing the generator voltage [6], is accompanied by changes of several TS characteristics (decrease of the breakdown voltage, smaller and broader spark current pulses). It also influences the breakdown mechanism via shortening of the streamer-to-spark transition time ( $\tau$ ) [7]. These frequency-dependent phenomena occur due to the various 'memory' effects (especially pre-heating, pre-ionization and gas composition changes by previous TS pulses) in the gap. The objective of this paper is to explore the changes of the breakdown mechanism in the TS discharge due to the memory effects in greater detail.

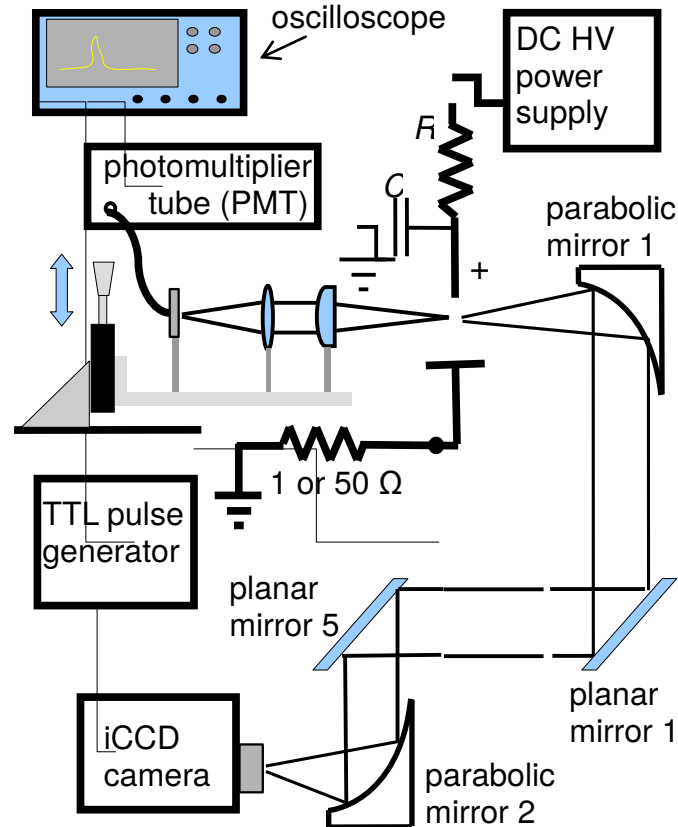


Fig. 1. Schematic of the experimental setup.

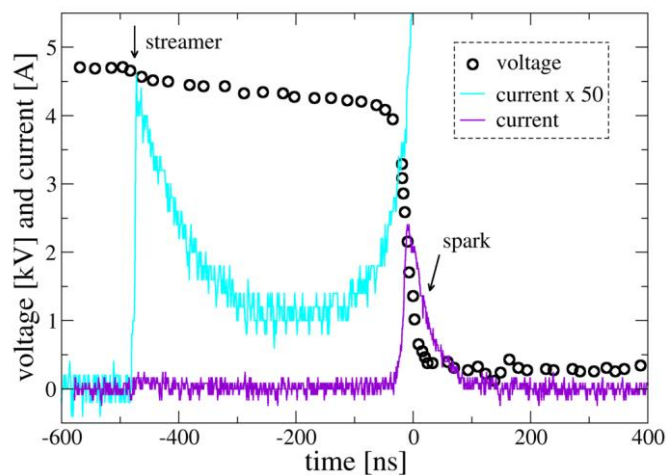


Fig. 2. Typical waveforms of transient spark discharge.

## 2. Experimental setup

Besides electrical measurements, various non-invasive optical spectroscopic methods are commonly used to investigate the plasma characteristics. Due to fast changes of plasma properties in short pulsed discharges such as TS, time-resolved techniques with  $\sim 1$  ns time resolution must be used. This can be accomplished by using intensified high speed CCD cameras [3, 7-9]. In order to achieve high spatial resolution, iCCD microscopy technique can be employed [10]. Fast streak cameras and cross-

correlation spectroscopy also provide valuable information about the evolution of transient discharge events [11, 12]. We performed time resolved imaging of the TS using a fast iCCD camera Andor iStar. Since the TS is a self-pulsing discharge, the synchronization between TS current pulses and the iCCD camera cannot be provided by an external trigger generator. Instead, the current signal of the TS itself was used to trigger the acquisition of the optical signal. The discharge current signal, linked to the 200 MHz digitizing oscilloscope Tektronix TDS2024, was measured on a 50  $\Omega$  or 1  $\Omega$  resistor shunts. The measurement of the discharge current on these shunts enabled us to synchronize the acquisition of the emission either with the beginning of the primary streamer (50  $\Omega$  shunt), or with the beginning of the spark (1  $\Omega$  shunt). As the current pulse reached a specified value, a TTL generator sent a voltage pulse to the iCCD camera to initiate the light acquisition. However, the initial  $\sim 45$  ns of the emission were impossible to acquire due to a delay caused by the trigger generator, the transmission time of the signal by BNC cables, and the camera insertion delay. For this reason we built an optical system consisting of two parabolic and five planar mirrors so that the light emitted by the discharge travels  $\sim 16$  m before it reaches the iCCD camera (Figure 1). The disadvantage of this approach was a complicated alignment of the optical system and weak signal. However, resulting delay of the optical signal enabled us to visualize the entire evolution of the streamer-to-spark transition in the TS.

Additionally to the iCCD temporal imaging, the spatiotemporal evolution of the discharges was analyzed by a photomultiplier tube (PMT). The light collection system was set on a micrometric translation stage to enable mapping of the light emission along the electrode's axis (2 points/mm). A cylindrical lens was used in the optical system to collect all the light in the plane perpendicular to the electrode's axis to avoid missing any discharge channel. The waveforms of the discharge current and PMT signal averaged over 128 individual discharges were recorded by the oscilloscope and subsequently processed and visualized. Processing of the PMT signals in the gap space and in time (2 ns resolution) enabled us to reconstruct the propagation of the streamer, secondary streamer and spark, with the visual output equivalent to a streak camera.

### 3. Results and Discussion

When the iCCD camera was synchronized with the beginning of the primary streamer current pulse, the propagation of the light from the anode to the cathode was observed. Figure 3 shows a sequence of the iCCD images obtained for the TS with  $f \approx 4$  kHz, gate width 2 ns,  $\sim 250$  accumulations,  $d = 5$  mm. The light propagation from the needle anode across the gap to the cathode in the time interval from 2 to 12 ns was appointed to the primary streamer. This streamer created a relatively conductive plasma bridge that after a certain delay enables transition to the spark. The spark itself is preceded by another light wave starting from the anode (time interval 16-36 ns), appointed to the so called secondary streamer. This name was given by Loeb who suggested it was a new ionization wave [13], but it is governed by the attachment processes [14]. The distribution of the attachment rate along the plasma filament generated by the primary streamer results in the reduced electric field  $E/N$  increase near the anode [14-17]. A decrease in the gas density  $N$  leads to the extension of this region with the increased  $E/N$ , i.e. the secondary streamer propagation, as was shown in the model of Bastien and Marode [14].

After the secondary streamer reaches the cathode, the spark may be launched. It takes a few tens of ns more before the actual spark appears (Figure 3). The earliest sparks appeared  $\sim 70$  ns after the beginning of the streamer, the highest probability of the spark onset was around 90 ns. The delay between the onset of spark and the moment when the secondary streamer reaches the cathode is probably because an additional heating of the plasma channel up to observed  $\sim 1000$  K is needed. This suggests that the final step in the breakdown is governed by the mechanism suggested by Marode [18]: the increase of  $T$  in the channel leads to an increase of the pressure, which is followed by a hydrodynamic channel expansion that empties the core of the channel and decreases the gas density  $N$ . For this reason, a reduced electric field strength  $E/N$  in the plasma channel increases and accelerates the electron-impact ionization. When the iCCD camera was synchronized with the beginning of the spark pulse, the emitted light appeared simultaneously in the entire plasma channel: no propagation of the light from the anode to the cathode was observed. We suppose that the  $E/N$  was high enough so that the ionization processes dominate along the entire discharge channel.

Fig. 3. Time resolved iCCD images of the TS discharge,  $f \approx 4$  kHz,  $d = 5$  mm, camera gate width 2 ns, accumulated over  $\sim 250$  pulses. The time delay with respect to the streamer initiation is indicated on individual frames. The brightness of images is shown relative (normalized) in each frame, the actual light emission of the secondary streamer is stronger than of the streamer, and that of the spark is much more intense than both streamer and secondary streamer.

The average streamer propagation velocity estimated from Fig. 3 was  $\sim 5 \times 10^7$  cm/s, the secondary streamer was only  $\sim 2$  times slower. More precise determination of these velocities, including their evolution along the gap was possible from the spatiotemporal reconstruction of PMT measurements (Figures 4 and 5). While the primary streamer accelerates as it approaches the anode, the secondary streamer slows down. The velocities of both primary and secondary streamers increase with  $f$  (Figure 6). According to the model of Bastien and Marode [14], the propagation of the secondary streamer can be explained by the increase of  $N$ . From faster propagation of the secondary streamers at higher TS frequencies we could thus deduce faster decrease of  $N$ . Assuming that decrease of  $N$  is caused by the heating of the gas inside the plasma channel, the heating should be faster at higher TS frequencies. This agrees with our previous experimental findings [7].

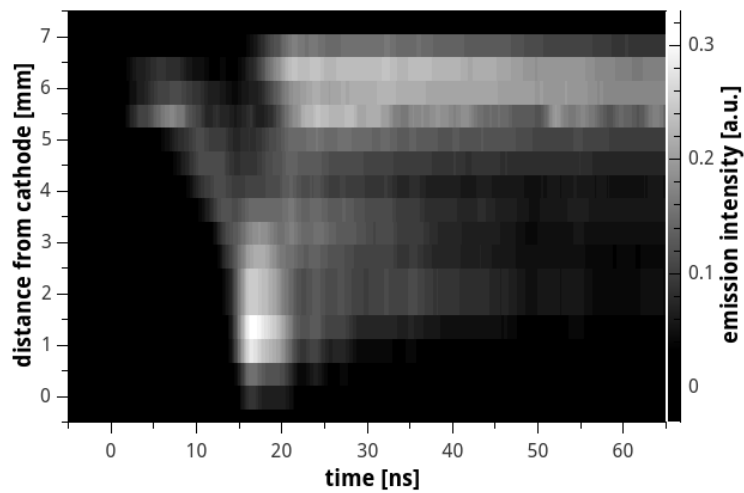


Fig. 4. Visualization of the streamer and secondary streamer from spatiotemporal reconstruction of the PMT signals (i.e. streak camera-like image), TS,  $f \approx 2.2$  kHz,  $d = 7$  mm.

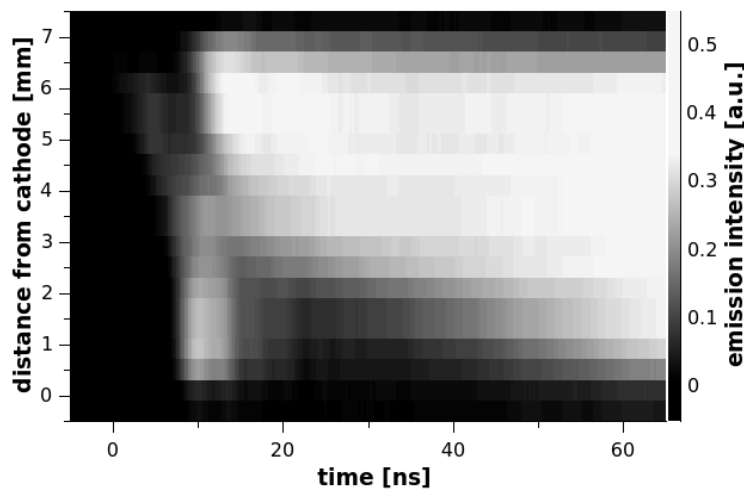


Fig. 5. Visualization of the streamer and secondary streamer from spatiotemporal reconstruction of the PMT signals (i.e. streak camera-like image), TS,  $f \approx 6$  kHz,  $d = 7$  mm.

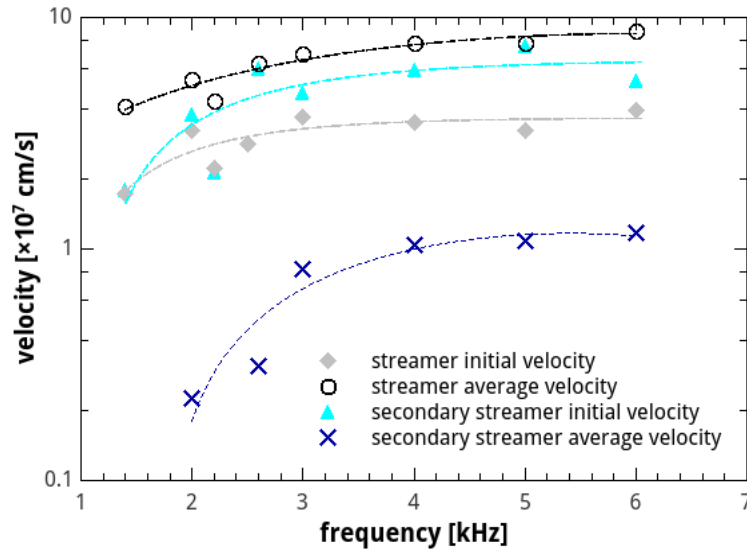


Fig. 6. Primary and secondary streamer propagation velocities as functions of TS repetition frequency.

The fast propagation of the secondary streamer through the whole gap could explain short streamer-to-spark transition times in TS at repetition frequencies above 3 kHz. At lower TS repetition frequencies, the initial velocity of the secondary streamer is also relatively high, but it does not propagate through the whole gap (Figure 4). These implies that the role of the secondary streamer on the breakdown increases with the increasing  $f$ . We suppose that this change in the streamer-to-spark transition mechanism is due to the memory effects induced by the previous TS pulses. The secondary streamer is governed by the attachment controlled processes, and the pre-heating can decrease the attachment rate due to decrease of  $N$  or by the acceleration of thermal detachment reactions. Accumulation of species such as atomic oxygen could increase the collisional detachment rate.

#### 4. Conclusions

We investigated the breakdown mechanism in the Transient Spark (TS) discharge in atmospheric pressure air, using time resolved imaging techniques. The TS is a self-pulsing discharge initiated by a streamer, with the subsequent short spark current pulse. The TS repetition frequency (1-10 kHz) can be controlled by the applied voltage. Despite this repetition frequency is not absolutely regular, we succeeded to observe the emission from the complete TS event. The iCCD camera was triggered by the rising slope of the streamer current pulse and the light was delayed by the system of mirrors. The disadvantage of this approach is complicated alignment of the optical system. Less effort was needed to obtain streak camera like pictures from set of optical emission intensity profiles measured by the PMT module. The signal from the PMT module was also synchronized by the rising slope of the streamer current pulse.

Based on the obtained images we suppose that the role of the so called attachment control processes [14] and secondary streamer on the breakdown mechanism increases with the increasing TS repetition frequency. The fast propagation of the secondary streamer through the whole gap at TS repetition frequencies above 3 kHz can explain the significant shortening of the streamer-to-spark transition time. The increasing propagation velocities of streamers and secondary streamers with increasing TS repetition frequency is probably due to a memory effect (pre-heating, pre-ionization, or gas composition changes) induced by previous TS pulses. Further research is required, including kinetic modeling, to verify this hypothesis and distinguish the respective contributors to the memory effect.



### Acknowledgement

Effort sponsored by the Slovak Research and Development Agency APVV-0134-12, and Slovak grant agency VEGA 1/0998/12.

### 5. References

- [1] Larsson A 1998 *J. Phys. D: Appl. Phys.* **31** 1100.
- [2] Naidis G V 2009 *Eur. Phys. J. Appl. Phys.* **47** 22803.
- [3] Pai D Z, Lacoste D A and Laux C O 2010 *Plasma Sources Sci. Technol.* **19** 065015.
- [4] Pai D Z, Lacoste D A and Laux C O 2010 *J. Appl. Phys.* **107** 093303.
- [5] Gerling T et al. 2013 *J. Phys. D: Appl. Phys.* **46** 145205.
- [6] Janda M, Martišovič V and Machala Z 2011 *Plasma Sources Sci. Technol.* **20** 035015.
- [7] Janda M, Machala Z, Niklová A and Martišovič V 2012 *Plasma Sources Sci. Technol.* **21** 045006.
- [8] Pai D Z, Stancu G D, Lacoste D A and Laux C O 2009 *Plasma Sources Sci. Technol.* **18** 045030.
- [9] Mihaila I, Ursu C, Gegiuc A and Popa G 2010 *J. Phys. Conf. Ser.* **207** 012005.
- [10] Šimek M, Ambrico P F and Prukner V 2011 *Plasma Sources Sci. Technol.* **20** 025010.
- [11] Marode E 1975 *J. Appl. Phys.* **46** 2005.
- [12] Brandenburg R, Grosch H, Hoder T and Weltmann K-D 2011 *Eur. Phys. J.- Appl. Phys.* **55** 13813.
- [13] Loeb L B 1965 *Electrical Coronas* (Univ. of California Press, Berkeley, California).
- [14] Bastien F and Marode E 1985 *J. Phys. D: Appl. Phys.* **18** 377.
- [15] Sigmond S R 1984 *J. Appl. Phys.* **56** 1355.
- [16] Marode E et al. 2009 *Plasma Phys. Control. Fusion* **51** 124002.
- [17] Ono R and Oda T 2007 *J. Phys. D: Appl. Phys.* **40** 176.
- [18] Marode E, Bastien F and Bakker M 1979 *J. Appl. Phys.* **50** 141.